cmgh
CELLULAR AND MOLECULAR GASTROENTEROLOGY AND HEPATOLOGY

ORIGINAL RESEARCH

Sorted-Cell Sequencing on HCC Specimens Reveals EPS8L3 as a Key Player in CD24/CD13/EpCAM-Triple Positive, Stemness-Related HCC Cells

Yu-Man Tsui,[1,2,*] Daniel Wai-Hung Ho,[1,2,*] Karen Man-Fong Sze,[1,2,*] Joyce Man-Fong Lee,[1,2] Eva Lee,[1,2] Qingyang Zhang,[1,2] Gary Cheuk-Hang Cheung,[1,2] Chung-Ngai Tang,[3] Victor Wai-Lun Tang,[4] Elaine Tin-Yan Cheung,[5] Irene Lai-Oi Lo,[6] Albert Chi-Yan Chan,[2,7] Tan-To Cheung,[2,7] and Irene Oi-Lin Ng[1,2]

[1]Department of Pathology, The University of Hong Kong, Hong Kong; [2]State Key Laboratory of Liver Research, The University of Hong Kong, Hong Kong; [3]Department of Surgery, Pamela Youde Hospital, Hong Kong; [4]Department of Pathology, Pamela Youde Hospital, Hong Kong; [5]Department of Pathology, Queen Elizabeth Hospital, Hong Kong; [6]Department of Surgery, Queen Elizabeth Hospital, Hong Kong; and [7]Department of Surgery, The University of Hong Kong, Hong Kong

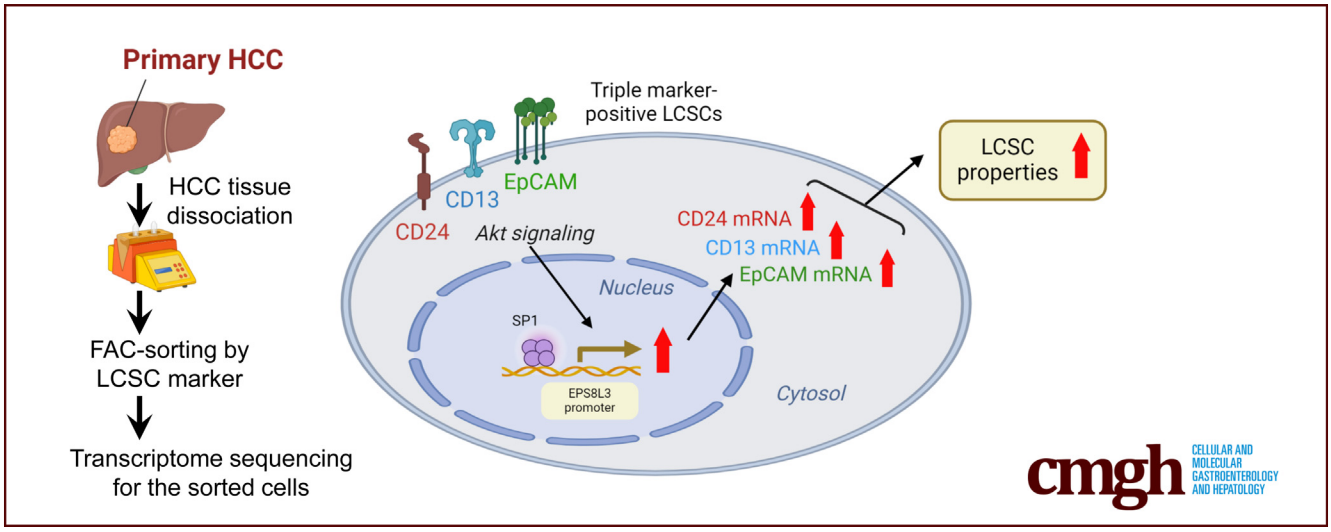

SUMMARY

Flow cytometric analysis of the expression of liver CSC markers in patients' HCCs identified CD24/CD13/EpCAM triple-positive stemness-related HCC cells. CD24/CD13/EpCAM triple positivity was associated with more advanced tumor stage in HCC. RNA sequencing on FAC-sorted patients' HCCs identified EPS8L3 expression that was associated with CD24/CD13/EpCAM triple positivity and SP1 driven.

BACKGROUND & AIMS: Hepatocellular carcinoma (HCC) is a heterogeneous cancer with varying levels of liver tumor initiating or cancer stem cells in the tumors. We aimed to investigate the expression of different liver cancer stem cell (LCSC) markers in human HCCs and identify their regulatory mechanisms in stemness-related cells.

METHODS: We used an unbiased, single-marker sorting approach by flow cytometry, fluorescence-activated cell sorting, and transcriptomic analyses on HCC patients' resected specimens. Knockdown approach was used, and relevant functional assays were conducted on the identified targets of interest.

RESULTS: Flow cytometry on a total of 60 HCC resected specimens showed significant heterogeneity in the expression of LCSC markers, with CD24, CD13, and EpCAM mainly contributing to this heterogeneity. Concomitant expression of CD24, CD13, and EpCAM was detected in 32 HCC samples, and this was associated with advanced tumor stages. Transcriptomic sequencing on the HCC cells sorted for these individual markers identified epidermal growth factor receptor kinase substrate 8-like protein 3 (EPS8L3) as a common gene associated with the 3 markers and was functionally validated in HCC cells. Knocking down EPS8L3 suppressed the expression of all 3 markers. To search for the upstream regulation of EPS8L3, we found SP1 bound to EPS8L3 promoter to drive EPS8L3 expression. Furthermore, using Akt inhibitor MK2206, we showed that Akt signaling–driven SP1 drove the expression of the 3 LCSC markers.

CONCLUSIONS: Our findings suggest that Akt signaling–driven SP1 promotes EPS8L3 expression, which is critical in maintaining the downstream expression of CD24, CD13, and EpCAM.

The findings provide insight into potential LCSC-targeting therapeutic strategies. *(Cell Mol Gastroenterol Hepatol 2024;18:101358; https://doi.org/10.1016/j.jcmgh.2024.05.006)*

Keywords: CD24/CD13/EpCAM1-Triple Positive; EPS8L3; Fluorescence-Activated Cell-Sorting; Liver Cancer Stem Cell.

Hepatocellular carcinoma (HCC) is a heterogeneous cancer with varying levels of liver cancer stem cells (LCSCs) and their associated markers,[1–4] which are associated with functional heterogeneity of the LCSCs.[5] These markers, such as CD13,[6] CD24,[7,8] CD44,[8] CD133,[9,10] and epithelial cell adhesion molecule (EpCAM)[11,12] are present in different combinations in HCC cells and indicate various subpopulations of LCSCs.[1–4] They are functioning markers driving different cell signaling pathways.[6,7,9,13] To develop effective therapies targeting these CSC populations, it is essential to understand their interacting roles and consensus downstream signaling pathways. However, studies on the concomitant expression of multiple LCSC markers in large HCC cohorts are scarce. Previous reports often had limitations such as improper gating, lack of marker-negative populations for comparison,[14–17] limited numbers of markers examined,[18–22] and small cohorts of HCC cases.[14–17] Therefore, further research is needed to analyze the combinations of various LCSC markers and their associated transcriptomes in the same set of HCC patient samples to better understand the downstream signaling pathways and potential therapeutic targets.

In this study, multiple LCSC markers were comprehensively and unbiasedly examined in the same cohort of HCC patient specimens by using flow cytometry to examine their expression at protein level. The results revealed significant heterogeneity in the expression of LCSC markers, with CD24, CD13, and EpCAM contributing most to this heterogeneity. Concomitant expression of these 3 markers was associated with more advanced tumor stage. To identify potential consensus signaling pathways related to these major LCSC markers, the transcriptomes of fluorescence-activated cell sorting (FACS) expression-high and expression-low HCC cells from patient samples were analyzed. Among the different individual LCSC marker-associated gene signatures, epidermal growth factor receptor kinase substrate 8-like protein 3 (EPS8L3) was identified as a common gene associated with these 3 markers. Using HCC cell line naturally having the combined expression of the 3 markers, the functional significance of triple-positive LCSCs and EPS8L3 in these subpopulations was validated. Knocking down EPS8L3 suppressed the expression of all 3 markers. Furthermore, exploration of the upstream regulatory mechanisms affecting EPS8L3 expression in the context of the 3 LCSC markers revealed that Akt signaling–driven Sp1 transcription factor (SP1) promoted EPS8L3 expression, which in turn drove the expression of CD24, CD13, and EpCAM. The findings provide insight into potential LCSC-targeting therapeutic strategies.

Results

Flow Cytometric Analysis on Patients' Surgically Resected Specimens Reveals Inter-patient Heterogeneity in the Expression of LCSC Markers, CD24, CD13, and EpCAM

In this study, a cohort of 100 HCC patient specimens prospectively collected between 2017 and 2019 were analyzed. After excluding cases that had significant tumor necrosis and insufficient viable CD45-negative malignant cells (Figure 1*A*), 60 cases were further examined for the expression of at least 1 LCSC marker using flow cytometry analysis (Figure 1*A*). Of these, 32 cases had enough viable cells for flow cytometry analyses of all 6 well-characterized LCSC markers (CD24, CD13, EpCAM, CD47, CD44, and CD133) previously reported by us and others (Figure 1*A*).

Among these 32 cases, flow cytometric analysis revealed varying proportions of positivity among these 6 LCSC markers (we defined positivity as >10% marker-positive cells) (Figure 1*A*). In addition, the means and medians for the percentages of cells positive for the different LCSC markers varied significantly (Figure 1*B*, Tables 1 and 2). This finding was consistent with the high degree of inter-tumoral heterogeneity of LCSCs demonstrated by using single-cell transcriptomics in previous studies.[2] CD47 was detected with a median percentage of positive cells as high as 93.4%, suggesting an almost invariable expression (Figure 1*B*, Table 2). CD47 serves as a "don't eat me" signal for normal immune regulation[23] and is ubiquitously expressed in human cells and human cancers including HCC.[15,24] In contrast, CD44 and CD133 were only detected in a minority (n = 1/32; 3.1%) of this HCC cohort, with the corresponding median of positive cells being 0% (Figure 1*B*, Table 2), implying that they might not be the primary LCSC markers contributing to the heterogeneity in LCSC populations in human HCC.

Because of technical constraints as mentioned above and a focus on identifying significant contributors to LCSC heterogeneity, we then concentrated on CD24, CD13, and EpCAM markers. Among the 32 cases, thirteen (40.6%) exhibited concomitant expression of all 3 markers in more

***Authors share co-first authorship.**

Abbreviations used in this paper: **ChIP, chromatin immunoprecipitation; DEG, differentially expressed gene; DMEM, Dulbecco modified Eagle medium; EGFR, epidermal growth factor receptor; EpCAM, epithelial cell adhesion molecule; EPS8L3, epidermal growth factor receptor kinase substrate 8-like protein 3; FACS, fluorescence-activated cell sorting; FBS, fetal bovine serum; FFPE, formalin-fixed paraffin-embedded; FPKM, fragments per kilobase per million; HCC, hepatocellular carcinoma; IgG, immunoglobin G; KD, knockdown; KLF5, Kruppel like factor 5; LCSC, liver cancer stem cell; MYO1A, myosin 1A; RIN, RNA integrity number; RT-qPCR, quantitative real-time polymerase chain reaction; shRNA, short hairpin RNA; SOX9, SRY-box transcription factor 9; SP1, Sp1 transcription factor; TCGA, The Cancer Genome Atlas.**

Most current article

2352-345X
https://doi.org/10.1016/j.jcmgh.2024.05.006

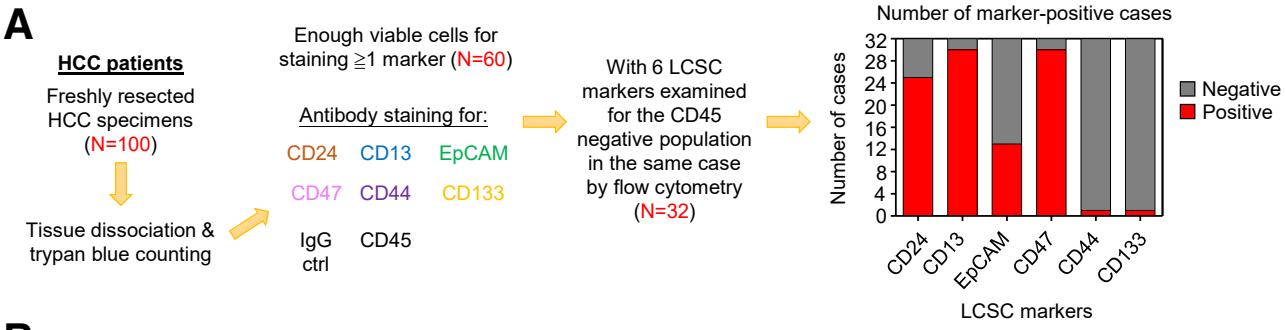

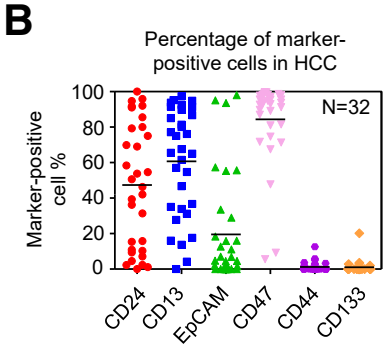

Marker-positive cell %	CD24	CD13	EpCAM	CD47	CD44	CD133
Mean	47.4%	60.7%	19.5%	84.4%	1.2%	1.1%
Median	48.5%	66.6%	4.7%	93.4%	0%	0%

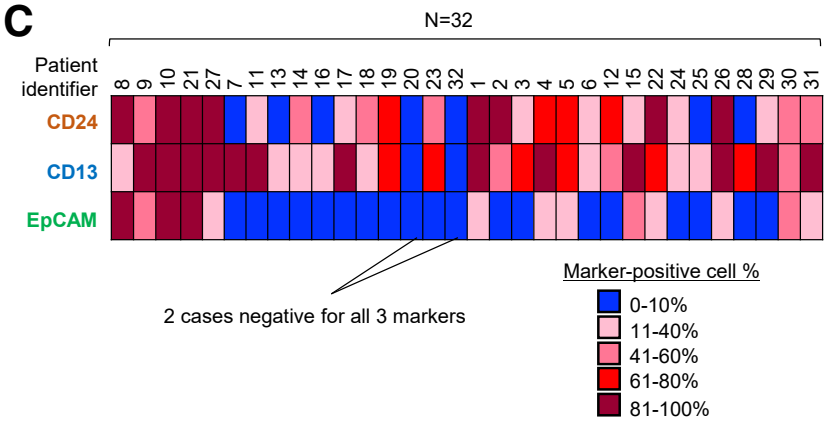

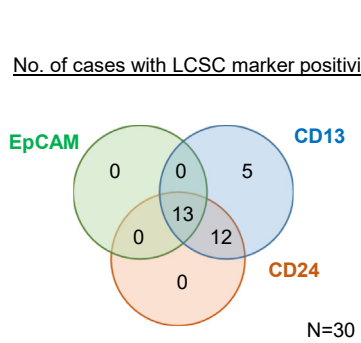

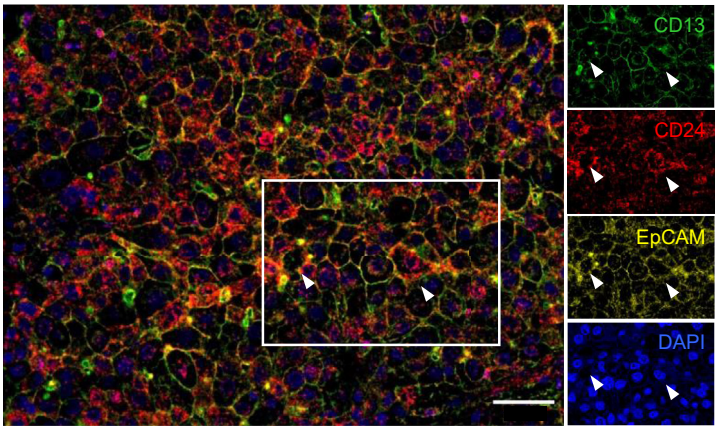

F

Clinicopathological features		Positive for all 3 markers	Positive for 1 or 2 markers	P-value
Tumor stage	I & II	8	18	.029
	III & IV	5	1	
Cellular differentiation	I & II	5	4	.427
	III & IV	8	15	
Venous invasion	Presence	9	11	.713
	Absence	4	8	
Tumor size	> 5cm	8	9	1.000
	≤ 5cm	5	10	

Table 1. Summary for Flow Cytometry Analysis for LCSC Markers CD24, CD13, and EpCAM for HCCs (N = 32)

Patient identifier	Percentage of marker-positive cells			CD24/CD13/EpCAM marker positivity status in HCC cases[a]
	CD24	CD13	EpCAM	
1	91.70%	86.70%	11.10%	Triple positive
4	69.00%	85.00%	16.00%	Triple positive
5	75.00%	76.10%	33.50%	Triple positive
8	91.00%	36.70%	95.10%	Triple positive
9	54.60%	94.90%	55.70%	Triple positive
10	100.00%	97.40%	93.60%	Triple positive
15	15.40%	81.40%	55.40%	Triple positive
21	85.50%	95.20%	98.00%	Triple positive
22	80.00%	75.00%	18.40%	Triple positive
26	92.00%	80.00%	12.70%	Triple positive
27	94.70%	91.50%	29.00%	Triple positive
30	53.80%	54.70%	57.40%	Triple positive
31	46.30%	92.50%	15.90%	Triple positive
2	95.90%	46.70%	7.00%	Double positive
3	36.20%	65.00%	6.90%	Double positive
6	10.30%	13.70%	2.30%	Double positive
11	31.40%	89.90%	0.00%	Double positive
12	69.90%	57.00%	4.80%	Double positive
14	50.60%	27.70%	0.00%	Double positive
17	39.40%	93.80%	0.00%	Double positive
18	58.40%	17.60%	0.00%	Double positive
19	79.30%	67.60%	0.00%	Double positive
23	42.00%	65.50%	0.00%	Double positive
24	15.80%	35.00%	2.00%	Double positive
29	10.90%	77.10%	4.50%	Double positive
7	1.10%	91.30%	0.00%	Single positive
13	4.50%	16.00%	0.00%	Single positive
16	2.40%	31.20%	0.00%	Single positive
25	9.40%	33.90%	4.60%	Single positive
28	7.10%	61.50%	1.60%	Single positive
20	2.30%	0.00%	0.00%	No positive
32	0.00%	4.20%	0.00%	No positive

[a]Positivity in the concerned marker is defined by >10% marker-positive cells in the CD45-negatively gated viable cell population.

than 10% of cells, whereas 2 were negative for all 3 markers (Figure 1*C* and *D*). This finding highlighted the significant contribution of CD24, CD13, and EpCAM to the heterogeneity of the LCSC populations in HCC and underscored their potential importance in further investigations and therapeutic strategies.

Figure 1. (***See previous page***). **Flow cytometry analyses and FACS by LCSC markers on HCC cells from dissociation of resected HCC specimens.** (*A*) Liver CSC markers flow cytometry and FACS strategy. One hundred HCC specimens were collected and processed, and 60 of them had enough viable cells for immunostaining for at least one LCSC marker for flow cytometry analyses. Thirty-two cases had all 6 LCSC markers examined. The proportion of cases with >10% marker-positive cells were 25/32, 30/32, 13/32, 30/32, 1/32, and 1/32 for CD24, CD13, EpCAM, CD47, CD44, and CD133, respectively. (*B*) Summary for HCC cases with the CD24, CD13, EpCAM, CD47, CD44, and CD133 examined by flow cytometry in a cohort of 32 cases. (*C*) Varying percentages of marker-positive cells for CD24, CD13, and EpCAM in HCC samples (N = 32). (*D*) Number of HCC cases with positivity (ie, >10% positive cells in CD45-negative live cell populations) in CD24, CD13, and EpCAM expression, respectively. (*E*) Multicolor immunofluorescence imaging on HCC. Representative images for patient #30 sample are shown (*green*, CD13; *red*, CD24; *yellow*, EpCAM; *blue*, DAPI). Scale bar = 50 μm. (*F*) Clinicopathologic correlation analysis for HCC cases with multiple LCSC markers (CD24, CD13, and EpCAM) positive (n = 32). Fisher exact test.

Table 2. Summary for Flow Cytometry Analysis for LCSC Markers CD47, CD44, and CD133 for HCCs (N = 32)

Case identifier	Percentage of marker-positive cells[a]		
	CD47	CD44	CD133
1	81.0%	5.9%	0.0%
4	89.2%	0.0%	0.0%
5	71.8%	3.7%	0.0%
8	98.0%	0.0%	0.0%
9	93.8%	0.0%	0.0%
10	87.0%	0.0%	0.0%
15	98.1%	0.0%	2.9%
21	98.7%	0.0%	0.0%
22	98.5%	0.0%	3.6%
26	95.6%	12.6%	0.0%
27	5.6%	5.2%	1.0%
30	89.8%	0.0%	0.0%
31	93.0%	0.0%	0.0%
2	92.7%	0.0%	0.0%
3	97.0%	0.0%	3.1%
6	97.8%	3.0%	0.0%
11	99.7%	0.0%	2.0%
12	98.0%	3.3%	20.2%
14	94.9%	0.0%	1.3%
17	95.5%	2.5%	0.0%
18	67.5%	0.0%	0.0%
19	91.3%	0.0%	0.0%
23	93.0%	2.0%	0.0%
24	47.8%	0.0%	0.0%
29	94.3%	0.0%	0.0%
7	71.4%	0.0%	0.0%
13	95.6%	0.0%	0.0%
16	99.3%	0.0%	0.0%
25	9.3%	0.0%	0.0%
28	74.7%	0.0%	0.0%
20	99.6%	0.0%	0.0%
32	81.5%	0.0%	0.0%

[a]Marker-positive cells in the CD45-negatively gated viable cell population.

Detection of CD24/CD13/EpCAM-Triple Positive LCSCs in Clinical HCC Samples and the Clinicopathologic Correlation of CD24/CD13/EpCAM-Triple Positivity

The presence of CD24/CD13/EpCAM-triple positive LCSCs in HCC was observed in the flow cytometry data (Table 1). Multiplex immunofluorescence performed on formalin-fixed paraffin-embedded (FFPE) sections of the corresponding HCC cases (Figure 1*E*) showed this triple positivity, with the staining present on the cell surfaces.

Among the 32 HCC cases analyzed, all but one were associated with chronic hepatitis B viral infection. When examining the clinicopathologic correlations, concomitant positivity of these 3 LCSC markers was significantly associated with more advanced tumor stages ($P = .029$, Fisher exact test) (Figure 1*F*), whereas no significant correlation was found between individual LCSC marker expression and advanced tumor stage (Table 3). There was no significant correlation between the positivity of all 3 LCSC markers or individual LCSC markers with the other pathologic parameters including cellular differentiation, venous invasion, and tumor size (Figure 1*F*, Table 3).

Transcriptomics Analysis of LCSC Marker-Sorted Cells in Clinical Samples Reveals Common Genes Associated With CD24/CD13/EpCAM-Triple Positive HCC Cells

Considering the LCSC heterogeneity primarily attributed to the expression of CD24, CD13, and EpCAM, we aimed to delineate the disparate and consensus mechanistic landscape driven by these 3 LCSC markers. We first gated the CD45-negative singlet live cell population to isolate cells with high and low expression of LCSC markers (including marker-negative cells) (Figure 2*A*). Because of the uncertainty of the proportion of cells positive for different combinations of markers, to obtain a substantial number of samples with enriched expression for each marker, we FAC-sorted the tumor cells for individual markers in a common cohort of 13 HCC cases that had robust expression for all 3 markers. In 11 of the 13 cases, the RNA extracted from the sorted cells for all 3 markers had good enough RNA quality (RNA integrity number [RIN] >6) and was subjected to transcriptome profiling (Figure 2*A*). For each marker, the transcriptomes of marker expression-high–sorted cells were compared with the corresponding marker expression-low counterparts (Figure 2*A*) to obtain the lists of differentially expressed genes (DEGs) for each marker. We identified a total of 833 up-regulated and 325 down-regulated genes that showed differential gene expression associated with single or multiple markers (Figure 2*B*). Surprisingly, there were very few genes that were concurrently up-regulated (n = 4) or down-regulated (n = 41) on enrichment of all 3 markers (Figure 2*C* and *D*). Specifically, 4 concurrently up-regulated LCSC marker target genes (Kruppel like factor 5 [KLF5], SRY-box transcription factor 9 [SOX9], EPS8L3, and myosin 1A [MYO1A]) were identified, and these genes displayed statistically significant up-regulation in marker expression-high tumor samples as compared with their corresponding marker expression-low counterparts ($P < .05$, unpaired t test) (Figure 2*E*).

Furthermore, in our in-house HCC RNA-sequencing cohort (N = 41 pairs), EPS8L3, MYO1A, and SOX9 expression was significantly higher in HCC tissues that had concomitantly high expression of CD24, CD13, and EpCAM than those without (Figure 3), validating some of the common genes identified from the FACS approach. We also overlapped the DEGs associated with multiple individual LCSC markers to Reactome pathway and gene ontology analyses (Figure 4*A*–*C*).

Table 3. Clinicopathologic Correlation Analysis for Individual LCSC Marker Expression (N = 32)

Clinicopathologic features		CD24			CD13			EpCAM		
		>10% positive	≤10% positive	*P* value	>10% positive	≤10% positive	*P* value	>10% positive	≤10% positive	*P* value
Tumor stage	I & II	20	6	1.000	24	2	1.000	10	16	.076
	III & IV	5	1		6	0		5	1	
Cellular differentiation (by Edmondson grading)	I & II	8	1	.640	9	0	1.000	6	3	.243
	III & IV	17	6		21	2		9	14	
Venous invasion	Present	16	4	1.000	19	1	1.000	10	10	.726
	Absent	9	3		11	1		5	7	
Tumor size	>5 cm	14	3	.995	15	2	.713	8	9	0.491
	≤5 cm	11	4		15	0		5	10	

EPS8L3 Is a Key Functional Gene Commonly Associated With Triple LCSC Marker-Positive HCC Cells

Among our cell line panel, Huh-7 was the only cell line that expresses all 3 LCSC markers (CD24, CD13, and EpCAM) and also the 4 common genes associated with these markers (KLF5, SOX9, EPS8L3, and MYO1A) at reasonable levels (Figure 5*A* and *B*). Hence it was used for further investigation. We knocked down the 4 common genes individually using 2 independent short hairpin RNA (shRNA) sequences targeting each respective gene in Huh-7 cells (Figure 5*C*). Although knocking down all 4 genes led to a statistically significant reduction in sphere formation (an in vitro test for self-renewal ability), it was the knockdown of EPS8L3 (Figure 5*D*) that had the most significant inhibitory effect (Figure 5*E* and *F*). In addition, we found that higher EPS8L3 expression was significantly associated with poorer overall survival rates in HCC patients, as according to The Cancer Genome Atlas (TCGA) data set and our in-house HCC patient cohort (Figure 5*G* and *H*). These findings suggest that EPS8L3 may play a role in the maintenance and expression of CD24, CD13, and EpCAM markers. Therefore, we focussed on EPS8L3 for further investigation in the context of CD24, CD13, EpCAM-expression background.

Concomitant Knockdown of the 3 LCSC Markers Suppresses Sphere Formation but Does Not Down-regulate All 4 Common Genes Including EPS8L3

We investigated the functional significance of CD24/CD13/EpCAM-triple positivity by simultaneously knocking down these 3 LCSC markers in Huh-7 cells, which naturally express these markers and the 4 common genes associated with them (Figure 5*A* and *B*). We confirmed the efficiency of the triple knockdown at the transcript levels using quantitative polymerase chain reaction (qPCR) and at the protein levels derived from the mean of intensity of the signals from flow cytometry analysis (Figure 6*A*). Our findings showed that simultaneous knockdown of the 3 markers significantly reduced the sphere formation (Figure 6*B*), suggesting that the triple-positive LCSC markers play an important role in maintaining the stemness of HCC cells. Intriguingly, although EPS8L3 was suppressed when the markers were concomitantly knocked down, the suppression was mild and not more than 2 folds (Figure 6*C*). This suggests that these 3 LCSC markers may not directly regulate the expression of EPS8L3, underscoring alternative regulatory network for EPS8L3 expression in the triple-marker positive LCSC population.

Akt Signaling–Driven SP1 Drives EPS8L3 Expression, Which Promotes the Expression of CD24, CD13, and EpCAM

Because knockdown of EPS8L3 suppressed sphere formation, we further investigated the upstream mechanisms controlling the expression of EPS8L3 in HCC cells. By combining TCGA, ENCODE chromatin immunoprecipitation (ChIP)-seq data, and INSECT2.0 data, in the context of liver (cancer) cells, we identified putative SP1-binding sites on the EPS8L3 promoter, suggesting SP1 is one of the potential transcription factors that may physically interact with particular regions of the EPS8L3 promoter (Figure 7*A*, left panel). We then performed dual luciferase reporter assays, which showed that SP1 overexpression increased EPS8L3 promoter activity (Figure 7*A*, middle panel). By mutating the predicted putative SP1-binding sites, we created EPS8L3 mutant promoters and observed significantly reduced activity of these mutant promoters (Figure 7*A*, right panel). The binding of SP1 to the EPS8L3 promoter was further validated by using ChIP, which showed that SP1 immunoprecipitation enriched the EPS8L3 promoter sequence (Figure 7*B*). Moreover, we found that knockdown of SP1 significantly suppressed EPS8L3 expression in Huh-7 cells (Figure 7*C*). In addition, there was a significant positive correlation between SP1 and EPS8L3 in the TCGA data set (Figure 7*D*). Because SP1 was reported to be activated by Akt signaling in HCC,[25] we tested whether suppressing Akt signaling would affect EPS8L3 expression. Our results showed that the Akt inhibitor, MK2206, reduced the EPS8L3 protein and mRNA levels (Figure 7*E* and *F*) and suppressed

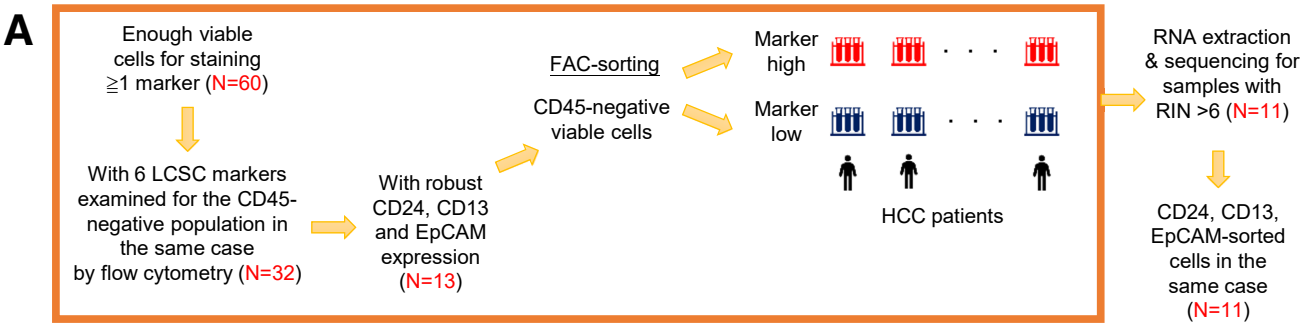

B

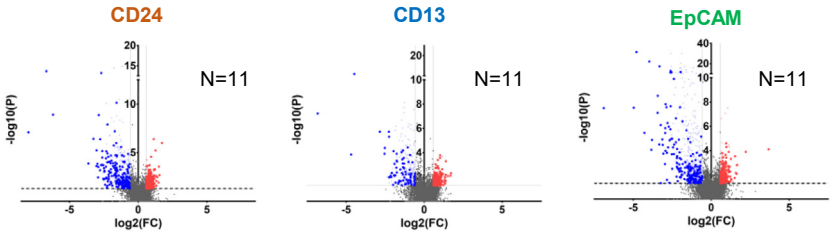

Criteria: Median FPKM > 0.5; Fold change >1.5-fold; P < 0.05

	LCSC markers	Up-regulated	Down-regulated
Numbers of DEGs in the sorted "marker-high" compared to the sorted "marker-low" cells	CD24	450	206
	CD13	206	79
	EpCAM	217	202

C

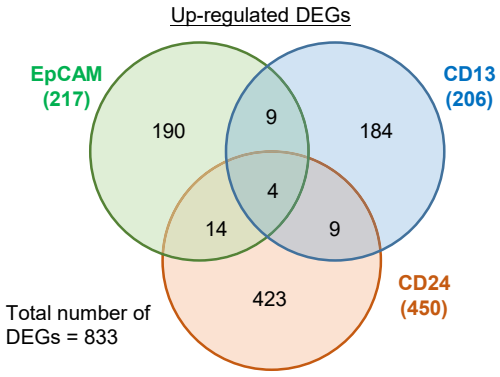

D

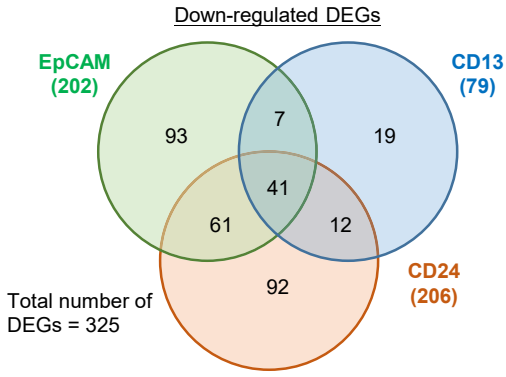

E

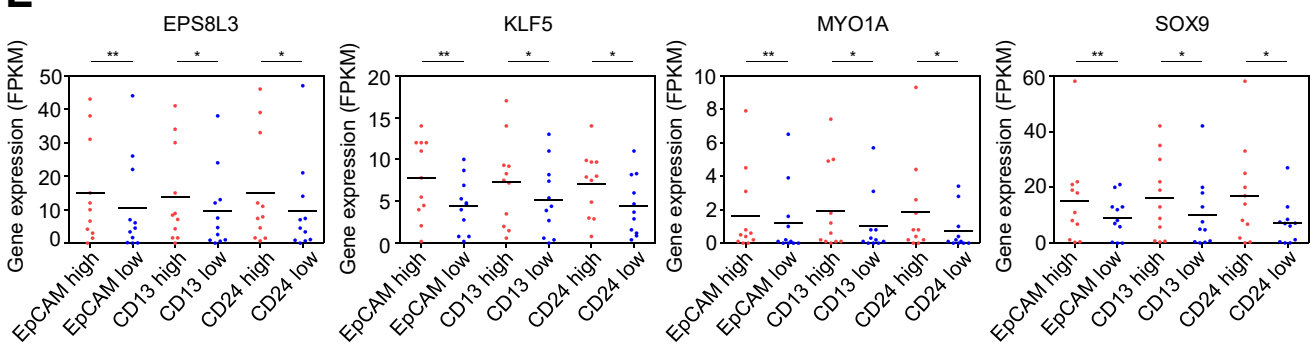

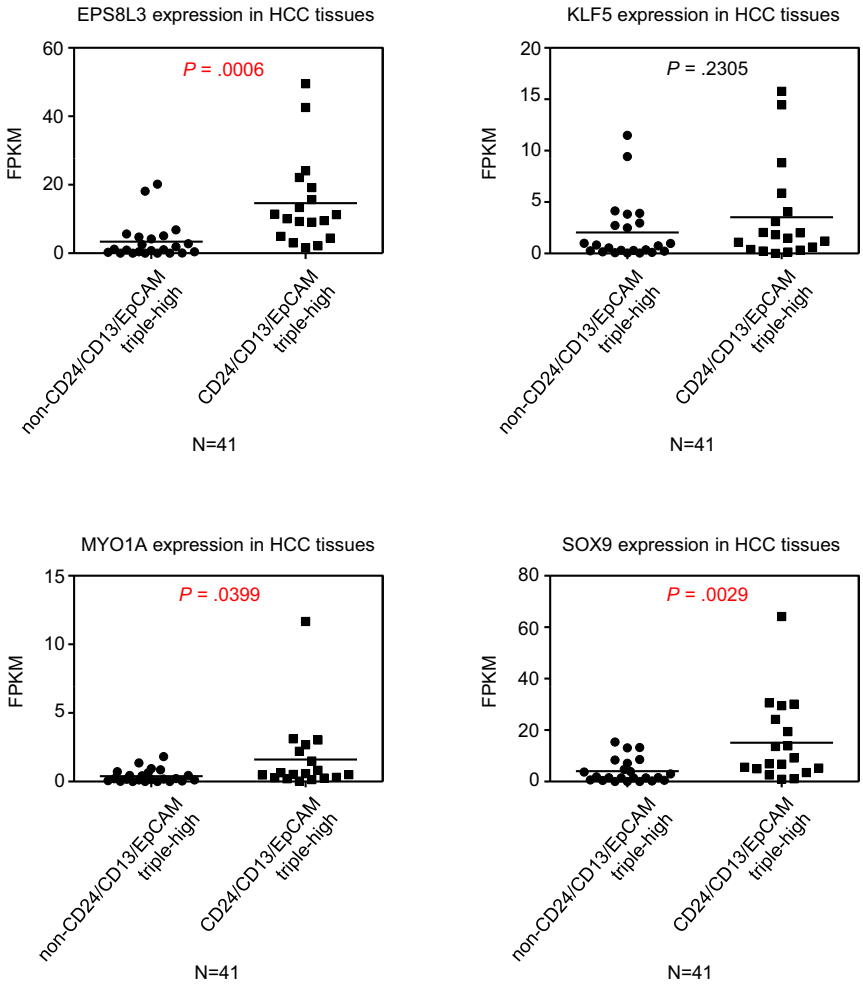

Figure 3. EPS8L3, MYO1A, and SOX9 expression was significantly higher in HCC tissues that have concomitantly high expression of CD24, CD13, and EpCAM than those tissues without. Expression with FPKM >5 was defined as high expression for the concerned LCSC markers in the HCC tissues.

SP1 transcriptional activity (Figure 7*G*). Knockdown of either SP1 or EPS8L3 (Figure 7*C* and *E*) inhibited proliferation of Huh7 cells (Figure 7*H*, left panel), resulting in increased cell doubling time (Figure 7*H*, right panel). The same was observed for Hep3B cells (Figure 8*A* and *B*). These findings support a positive role of Akt signaling and its driven SP1 activation and transcriptional activity in promoting EPS8L3 expression. Furthermore, knocking down EPS8L3 suppressed the expression of all these 3 LCSC markers (Figure 8*C*) in Huh-7, whereas overexpressing EPS8L3 in a EPS8L3-low HCC cell line, HepG2, showed the opposite effects (Figure 8*D*). This suggests that EPS8L3 is critical for maintaining LCSCs and regulating the downstream expression of the 3 LCSC markers.

Figure 2. (***See previous page***). **Transcriptomic analysis of CD24, CD13, and EpCAM-sorted HCC cells from resected HCC specimens to identify consensus landscape associated with the 3 LCSC markers.** (*A*) FAC-sorted pairs of marker-high and marker-low cells for individual CSC markers and RNA sequencing performed on those paired RNA samples with good enough quality (RIN >6). The CD45-negative singlet live cell population having the highest 20% staining intensity and being positive for the concerned fluorochrome was regarded as the marker expression-high cells, whereas the population with 2-fold lower intensity or negative staining was regarded as marker expression-low cells. We ultimately had 11 cases with paired FAC-sorted cells that gave RNA samples of good enough RNA quality (RIN >6.0) for the 3 respective LCSC markers in the same case. (*B*) Multiple DEGs between marker-sorted high vs marker-sorted low cells were found for the 3 concerned LCSC markers. (*C*) A total of 833 up-regulated genes in single or multiple marker-high cells than the marker-low counterparts. Overlapping of DEGs up-regulated in individual LCSC marker-high sorted cells resulted in 4 genes commonly up-regulated in marker sorted-high versus marker sorted-low cells for the multiple LCSC markers EpCAM, CD13, and CD24 in various combinations. (*D*) A total of 325 down-regulated genes in single or multiple marker-high cells than the marker-low counterparts. Overlapping of DEGs down-regulated in individual LCSC marker-high sorted cells resulted in 41 genes commonly down-regulated in marker sorted-high versus marker sorted-low cells for the multiple LCSC markers EpCAM, CD13, and CD24 in various combinations. (*E*) EPS8L3, KLF5, MYO1A, and SOX9 were the common DEGs found from pairwise analysis of CD24, CD13, EpCAM-sorted samples. ***$P < .001$; **$P < .01$; *$P < .05$; unpaired *t* test.

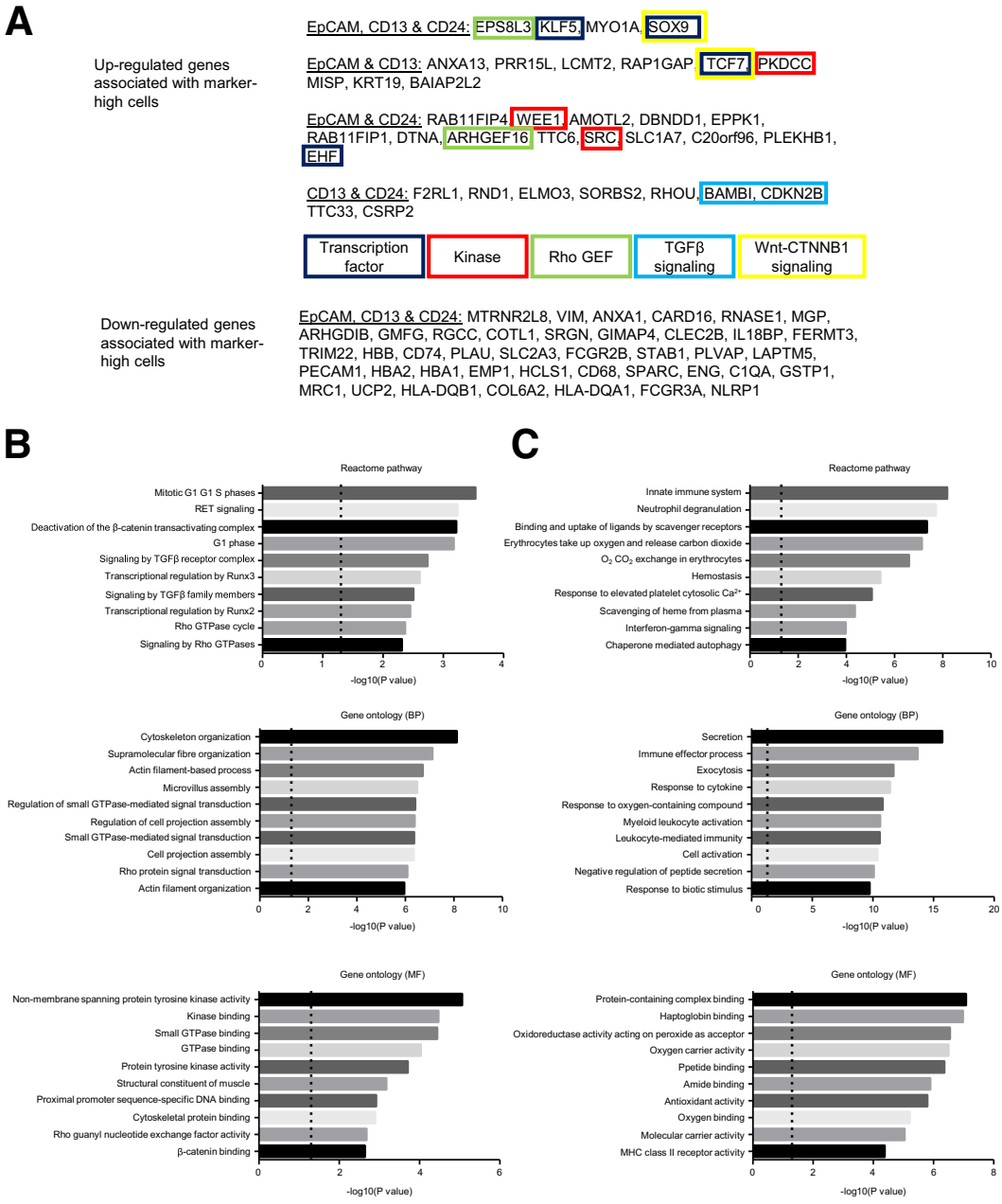

Figure 4. Reactome pathway and gene ontology analyses for the transcriptome of a cohort of FAC-sorted pairs for all 3 LCSC markers, CD24, CD13, and EpCAM. (*A*) Within a cohort of 11 cases with paired FAC-sorted cells RNA samples of good enough RNA quality (RIN >6.0) for all the 3 respective LCSC markers, CD24, CD13, and EpCAM, in the same case, overlapping of DEGs up-regulated in individual LCSC marker-high sorted cells resulted in a list of 4 genes commonly up-regulated in marker sorted-high versus marker sorted-low cells for the multiple LCSC markers in various combinations (*upper panel*). Overlapping of DEGs down-regulated in individual LCSC marker-high sorted cells resulted in a list of 41 genes commonly down-regulated in marker sorted-high versus marker sorted-low cells for the multiple LCSC markers EpCAM, CD13, and CD24 in various combinations (*lower panel*). (*B*) Reactome pathway analyses and gene ontology analyses for biological processes (BP) and molecular functions (MF) for the up-regulated DEGs enriched in marker-high cells for ≥2 out of the 3 concerned LCSC markers. (*C*) Reactome pathway analyses and gene ontology analyses for biological processes (BP) and molecular functions (MF) for the down-regulated DEGs enriched in marker-high cells for ≥2 out of the 3 concerned LCSC markers.

Discussion

In this study, we performed a comprehensive, unbiased examination of the expression of multiple LCSC markers in patients' resected HCC specimens, revealing different percentages of marker-positive HCC cells across these cases and highlighting the inter-tumoral heterogeneity in cancer stemness. This underscores the importance of studying LCSC subpopulations by using a sorting approach rather

A

Cell line	CD24	CD13	EpCAM	CD133	CD44
Huh-7	+	+	+	+	-
Hep3B	+	+	+	+	-
PLC/PRF/5	+	+	-	-	-
MHCC-97L	+	+	-	-	+
MIHA	-	+	+	-	-
HepG2	-	+	+	+	-

B

Description	FPKM values						
	CD24	EpCAM	ANPEP (CD13)	EPS8L3	KLF5	MYO1A	SOX9
Huh-7	475.08	11.37	30.10	13.61	8.01	1.07	24.40
Hep3B	387.36	157.18	24.56	15.22	3.61	0.03	32.40
PLC/PRF/5	120.92	0.97	32.67	5.08	32.17	0.34	4.78
MHCC-97L	7.43	0.13	1.21	8.60	14.89	0.22	8.52

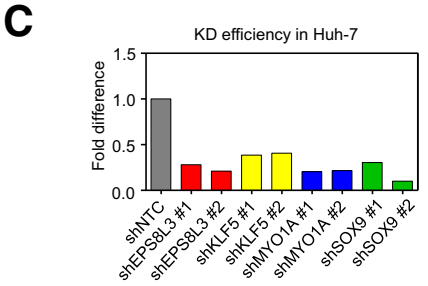

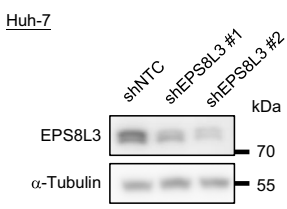

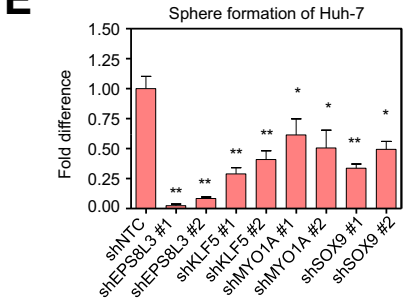

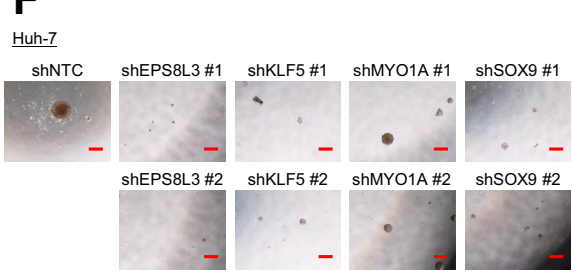

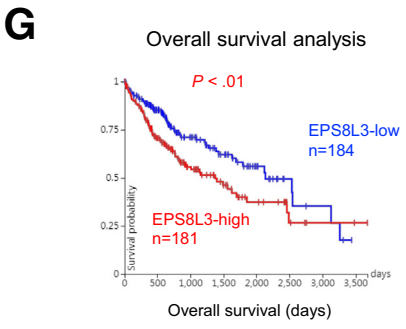

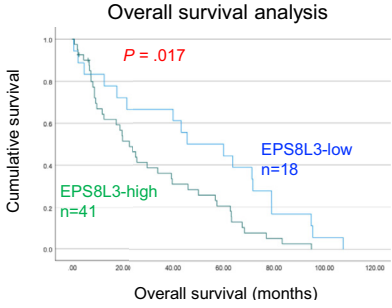

Figure 5. Study of the 4 identified genes associated with sorted CD24-, CD13-, EpCAM-high HCC cells. (*A*) Positivity of the various LCSC markers in various HCC cell lines and MIHA cells. (*B*) The FPKM values indicating mRNA expression for the 3 LCSC markers, CD24, CD13, and EpCAM, and the 4 identified genes in various HCC cell lines. (*C*) Knockdown (KD) efficiency of the 4 identified genes (EPS8L3, KLF5, MYO1A, and SOX9) by 2 respective independent shRNA sequences in Huh-7 cells was determined by RT-PCR. (*D*) KD of EPS8L3 in Huh-7 cells at protein level as determined by Western blot. (*E* and *F*) Sphere formation assay for Huh-7 cells on stable knockdown of EPS8L3, KLF5, MYO1A, and SOX9. Scale bar = 200 μm. (*G*) Overall survival analysis for EPS8L3 expression in TCGA data set by Xena Browser. Cases with EPS8L3 expression greater than the median in the TCGA cohort were defined as EPS8L3-high cases. (*H*) Overall survival analysis for EPS8L3 expression detected by qPCR in our in-house patient cohort. Cases with greater than 2-fold higher EPS8L3 expression in HCC than the corresponding NT were defined as EPS8L3-high cases. $^{**}P < .01$; $^{*}P < .05$; ns, not significant; paired *t* test.

than analyzing tumor bulk samples. Currently, there are 2 main methods to investigate the transcriptome associated with LCSC marker-positive cells: single-cell RNA sequencing and the traditional FACS approach. However, considering the potential inconsistency between LCSC marker protein and transcript expression, as well as the unknown threshold of transcript levels required for corresponding protein expression in clinical samples, in this study, we chose to base our analysis on LCSC marker protein levels with flow cytometry and sorting marker-high and marker-low HCC cells using FACS.

To our knowledge, most existing studies have used various LCSC markers to sort cells from either cultured HCC cells or spheroid cultures for functional or

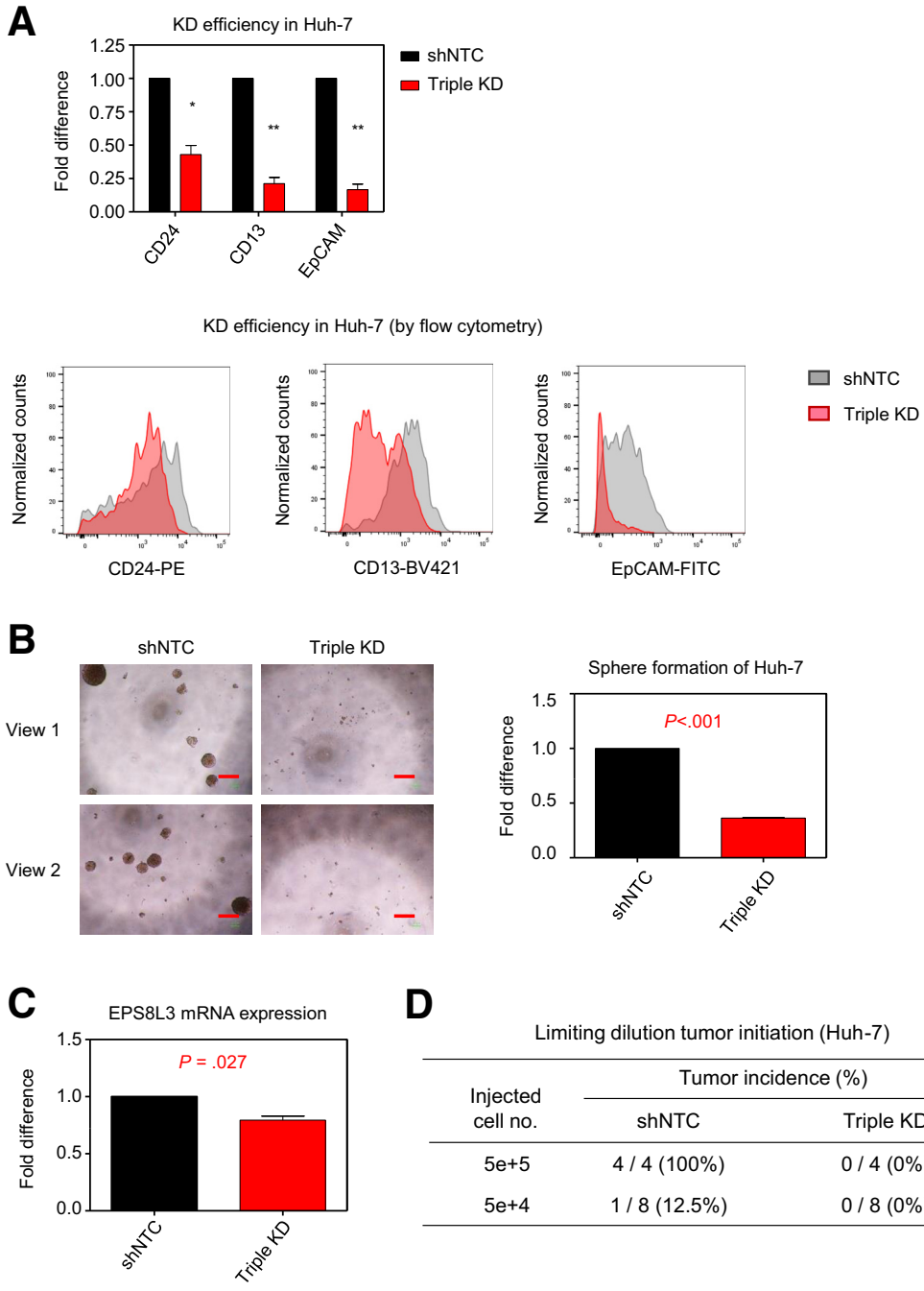

Figure 6. Concomitant triple knockdown of the 3 LCSC markers suppressed sphere formation. (*A*) KD efficiency of CD24, CD13, and EpCAM in triple KD Huh-7 cells was verified by qPCR (*left panel*) and flow cytometry in terms of mean of intensity (MOI) of the respective signals (*right panels*) for the respective LCSC markers. (*B*) Sphere formation assays for Huh-7 cells with concomitant triple knockdown of the 3 LCSC markers. Scale bar = 200 μm. (*C*) Expression of EPS8L3 was determined by RT-PCR in Huh-7 cells with triple KD of the 3 LCSC markers. (*D*) In vivo tumorigenicity assay using limiting dilution assay. $^{**}P < .01$; $^{*}P < .05$; ns, not significant; paired *t* test.

D

Limiting dilution tumor initiation (Huh-7)

Injected cell no.	Tumor incidence (%)	
	shNTC	Triple KD
5e+5	4 / 4 (100%)	0 / 4 (0%)
5e+4	1 / 8 (12.5%)	0 / 8 (0%)

mechanistic investigations into signaling pathways of different LCSC markers.[18–22] In contrast, our study performed cell sorting and transcriptome profiling directly on HCC clinical specimens, providing a more accurate representation of the in vivo situation and potentially leading to more clinically relevant findings. Furthermore, our study demonstrated that LCSCs in patient HCC specimens did not necessarily have similar combinations of LCSC marker expression as compared with HCC cell lines, emphasizing the value of using primary HCC specimens rather than HCC cell lines for FACS-based LCSC studies. However, because of the practical constraints in sorting all possible combinations of the concerned LCSC markers, with possible vast numbers of permutations of combinations, we adopted an approach of single marker-based sorting for multiple LCSC markers in the same set of clinical samples from an HCC patient cohort. Indeed, in our sample cohort, we found that the expression of individual LCSC markers was not mutually exclusive; in fact, they demonstrated a considerable degree of expression concurrency. We found that a significant proportion of HCC cases had non-negligible proportions of marker-positive cells for multiple LCSC

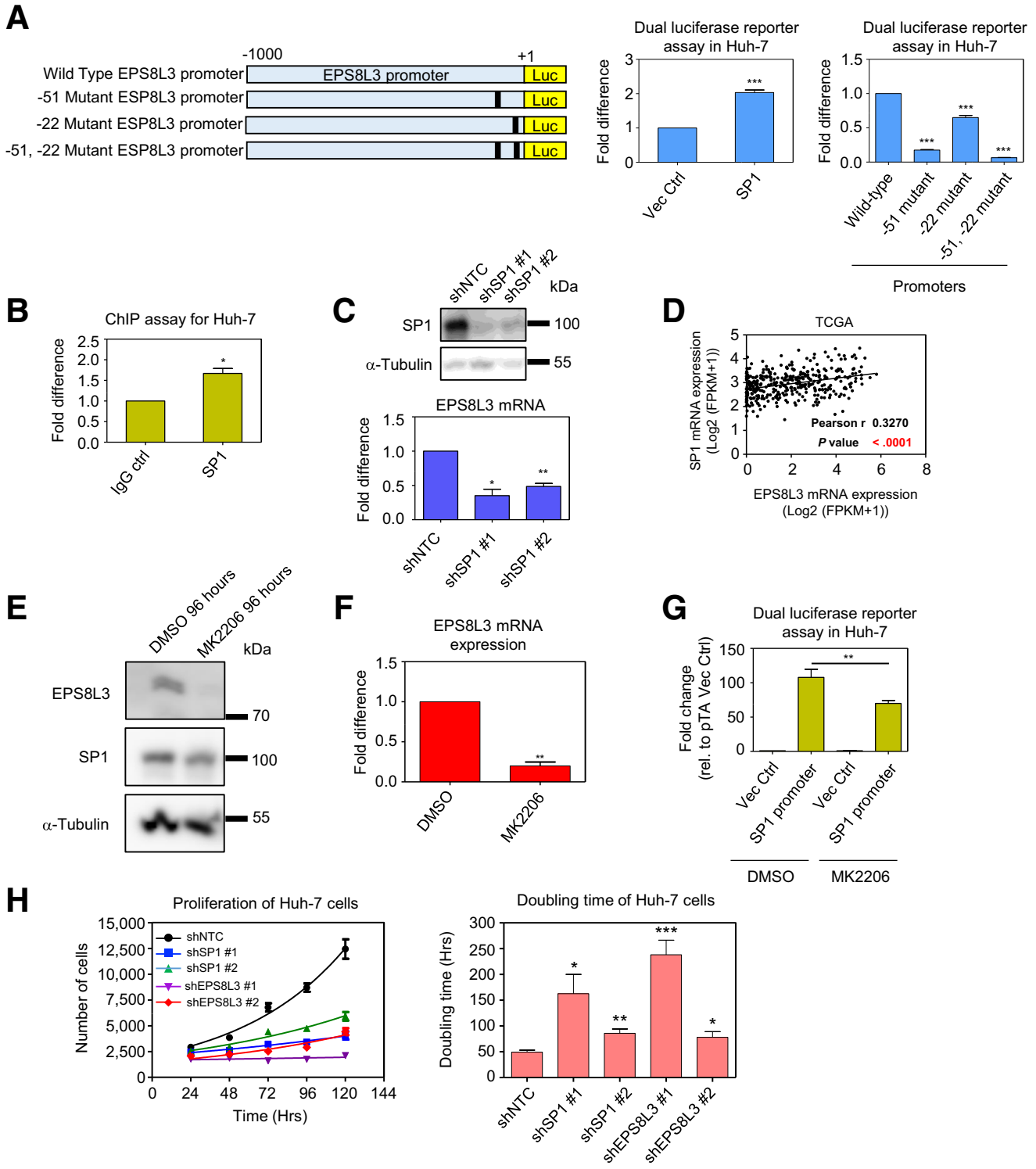

Figure 7. EPS8L3 expression driven by Akt signaling driven–SP1 to promote the 3 LCSC marker expression. (*A*) EPS8L3 promoter activity as determined by dual-luciferase reporter assay on SP1 overexpression in Huh-7. (*B*) ChIP assays by using anti-SP1 antibody for EPS8L3 promoter in Huh-7. (*C*) Stable SP1 KD suppressed EPS8L3 expression in Huh-7. (*D*) Positive correlation between SP1 and EPS8L3 in TCGA data set. (*E* and *F*) AKT inhibitor MK2206 (96-hour treatment) suppressed EPS8L3 expression in Huh-7. (*G*) AKT inhibitor MK2206 suppressed the transcription activity of SP1 in Huh7 cells, as compared with vector control (pTA-pGL3 Basic). The reporter construct for SP1 promoter was 3X SP1/pTA-pGL3 Basic. The transfected cells were subjected to 24-hour 10 μmol/L MK2206 treatment (n = 6). (*H*) Either SP1 or EPS8L3 KD by 2 respective independent shRNA sequences suppressed Huh-7 cell proliferation, thus increasing the doubling time. $^{**}P < .01$; $^{*}P < .05$; ns, not significant; paired *t* test.

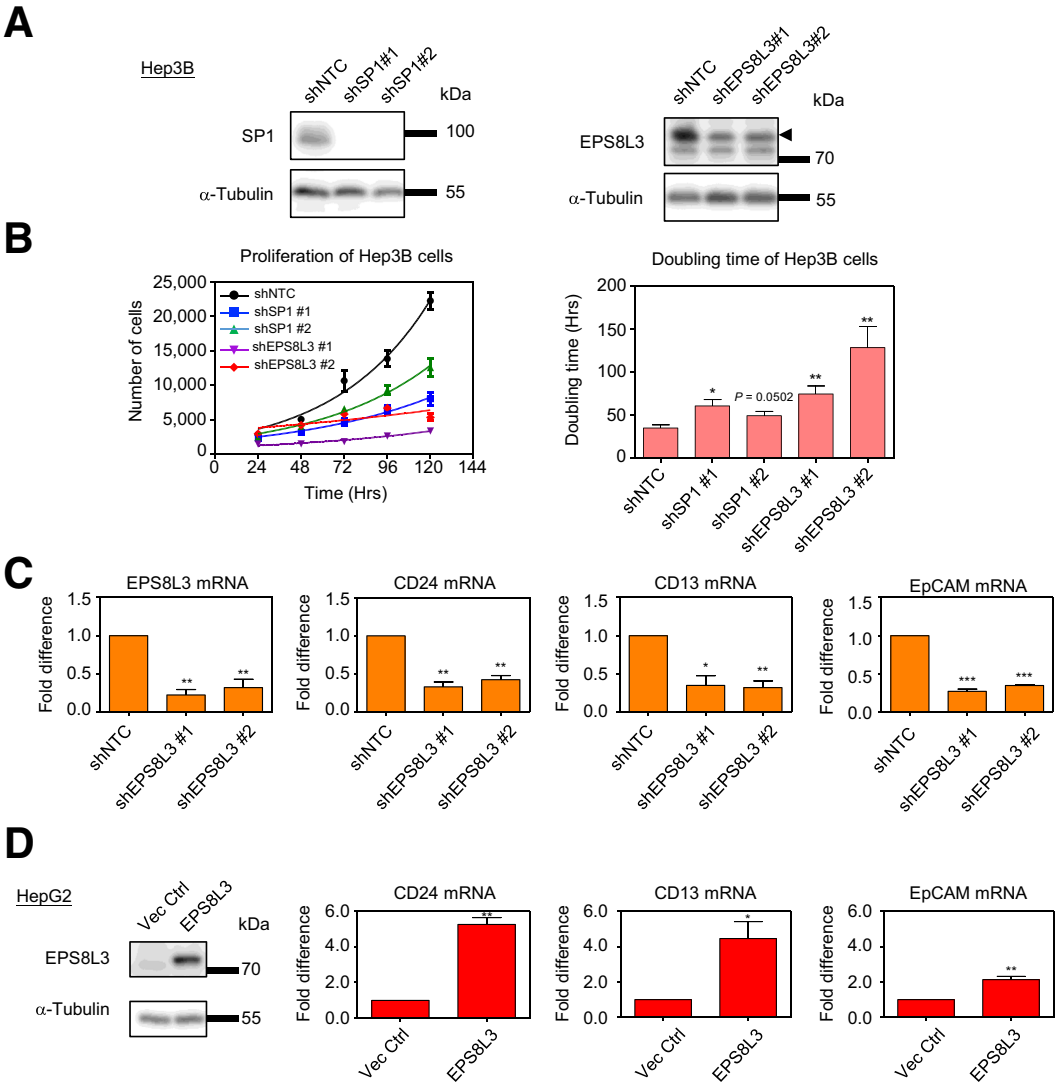

Figure 8. Study about SP1 and EPS8L3 by KD approaches in Hep3B. (*A*) KD of SP1 or EPS8L3 in Hep3B cells. (*B*) Either SP1 or EPS8L3 KD by 2 respective independent shRNA sequences suppressed Hep3B cell proliferation, thus increasing the doubling time. (*C*) KD of EPS8L3 suppressed the expression of the 3 LCSC markers (CD24, CD13, EpCAM) in Huh-7. (*D*) Stable overexpression of EPS8L3 promoted the expression of the 3 LCSC markers (CD24, CD13, EpCAM) in HepG2. $^{**}P < .01$; $^{*}P < .05$; ns, not significant; paired *t* test.

markers. Furthermore, we observed frequent concurrent expression among CD24, CD13, and EpCAM, as well as the presence of CD24/CD13/EpCAM triple-positive LCSCs in our human HCC samples and HCC cell lines. Intriguingly, within the same cohort, the concurrent positivity for these 3 LCSC markers showed a significant correlation with advanced tumor stage.

Concurrent triple knockdown of CD24, CD13, and EpCAM significantly suppressed sphere formation, suggesting that the participation of multiple LCSC markers, instead of single markers, may drive the aggressive features of LCSCs. This exemplifies the practical difficulty in treatments targeting LCSCs and the limitation in effectively eliminating LCSCs by targeting only a single marker and the associated downstream signaling pathway. To this end, we focused on the transcriptomes of LCSCs sorted by these 3 LCSC markers to investigate whether there were common regulatory mechanisms for multiple LCSC markers. This approach could overcome the challenges posed by the complex interplay between different LCSC markers in HCC. From the comparison of the transcriptomes of marker-high and marker-low samples, we identified DEGs associated with marker-high HCC cells for each individual marker. However, our results revealed a seemingly low degree of consensus among the underlying gene expression signatures for different LCSC markers. This may indicate the great diversity of signaling pathways and molecular mechanisms involved in their regulation, highlighting the complex and diverse signaling landscape associated with different LCSC markers in HCC. However, we were still able to identify some up-regulated genes (EPS8L3, KLF5, SOX9, and MYO1A) that were concurrently

Table 4. Antibodies and Dye Used for Flow Cytometry and FACS and Antibodies Used for Western Blots, ChIP Assay, and Other Reagents

Antibodies/dye	Manufacturer of antibodies	Item number
7AAD	Becton Dickinson	559925
IgG-BV421	Becton Dickinson	562438
CD24-BV421	Becton Dickinson	562789
CD47-BV421	Becton Dickinson	563760
EpCAM-BV421	Becton Dickinson	563180
CD13-BV421	Becton Dickinson	562596
IgG-VioBright FITC	Miltenyi Biotec	130-104-575
CD133/2-VioBright FITC	Miltenyi Biotec	130-104-273
IgG-PE	Becton Dickinson	555749
CD45-PE	Becton Dickinson	555483
IgG-VioBlue	Miltenyi Biotec	130-094-670
CD44-VioBlue	Miltenyi Biotec	130-113-337
Anti-EPS8L3	LifeSpan BioSciences	LS-C167794
Anti-SP1	Abcam	Ab 13370
Anti-α-Tubulin	Sigma-Aldrich	T9026
Normal rabbit IgG	Santa Cruz Biotechnology	sc-2027
MK2206	Selleckchem	S1078

associated with EpCAM, CD13, and CD24. The former 3 genes have been reported to confer HCC proliferation and cancer stemness properties.[26–29] Especially for EPS8L3, it has been reported to promote cell proliferation,[29–32] cell migration and invasion,[30–32] tumor growth,[30,32] metastasis,[30] and sorafenib resistance.[32] On the other hand, MYO1A has a more elusive role in HCC.[33] In fact, MYO1A did not have a clear functional role in sphere formation of HCC cells in our study. In contrast, knockdown of EPS8L3 showed the most significant reduction in sphere formation. Interestingly, knockdown of EPS8L3 suppressed CD24, CD13, and EpCAM expression. The underlying molecular mechanisms for the functional role of EPS8L3 have been widely studied by others. EPS8L3 was required for the expression of CCNA2, CCNB1, CDK1, BIRC5 proteins that promote cell division.[32] It was believed that EPS8L3 activated cell cycle progression via increasing c-myc, CDC25A, CCNE, CCNA2, and CCNF protein expression.[32] Furthermore, EPS8L3 promoted epidermal growth factor receptor (EGFR) dimerization and internalization to drive subsequent EGFR signaling, as exemplified by the EPS8L3-induced phosphorylation of EGFR and MEK.[30] Another study found that EPS8L3 promoted Akt and FOXO protein phosphorylation, suggesting a role of Akt/FOXO axis in promoting cyclinD1 expression on EPS8L3 overexpression.[29,31] We further investigated additional/alterative upstream regulation of EPS8L3 and identified that SP1 bound to EPS8L3 promoter to enhance EPS8L3 expression. Although there is statistically significant positive correlation between EPS8L3 and SP1 expression in the TCGA cohort of HCC samples, interestingly, there are still certain portion of cases showing high EPS8L3 but relatively low level of SP1. This indicates that SP1 is not the sole regulator of EPS8L3, and there is additional regulation of EPS8L3 other than SP1, pending further discovery in future studies. Because Akt signaling has been demonstrated to be the upstream driver of SP1 transcriptional activity in multiple studies,[25,34] we performed further experiments using Akt inhibitor MK2206 and validated that Akt signaling–driven SP1 could drive EPS8L3 expression. Although Akt pathway has multiple downstream targets, as reviewed previously,[35] here we are looking specifically at the Akt-SP1-EPS8L3 axis. On the other hand, how EPS8L3 drives the expression of these 3 LCSC markers is interesting but out of the scope of this study and is worthy for further study.

Altogether, by using this sorting appraoch, we identified EPS8L3 to be associated with CD24/CD13/EpCAM-triple LCSC marker positivity. Akt signaling–driven SP1 promoted EPS8L3 expression, which drove CD24, CD13, and EpCAM expression in the context of CD24/CD13/EpCAM-triple positivity. Such triple positivity in HCC tumors was associated with advanced tumor stage.

In summary, our findings suggest that Akt signaling–driven SP1 promotes EPS8L3 expression, which is critical in maintaining the downstream expression of CD24, CD13, and EpCAM. The findings provide insight into potential LCSC-targeting therapeutic strategies.

Materials and Methods

Clinical Specimens and Tumor Tissue Dissociation

A total of 100 HCC patients' resected surgical specimens were collected from Queen Mary, Queen Elizabeth, and Pamela Youde Eastern Hospitals with approval by the joint Institutional Review Board of the University of Hong Kong/Hospital Authority Hong Kong

Table 5. Primers or Oligos for Cloning, shRNA Sequences, and RT-qPCR

Primer names	Sequences (5' to 3')
For cloning promoters to make the reporter constructs	
EPS8L3p-1k-BglIIF	AGATCTGCTGAGATATCCTGGGATAGTTCC
EPS8L3p+1-HD3R	AAGCTTTGGCCACAGGCAGAGCCTGCC
EPS8L3p-22M-HD3R	AAGCTTTGGCCACAGGCAGATTTTTTTTTTGATGAGGTTACAGAG
EPS8L3p-51MF	GAGTCCAAAGAGCAAAAAAATAAATGCCTCTGTAACCTC
EPS8L3p-51MR	GAGGTTACAGAGGCATTTATTTTTTTGCTCTTTGGACTC
For ChIP-qPCR assay	
EPS8L3-121ChipF	CGCAGGTCCAGGTTGATGTT
EPS8L3-11ChipR	AGAGCCTGCCTTTGATGAGG
EPS8L3-57ChipFAM	AGAGCACAGGCGTGGCTGCC
For cloning shRNA sequences	
shEPS8L3#1F	CCGGGGAGCCAGCTACTTCGCATAACTCGAGTTATGCGAAGTAGCTGGCTCCTTTTTG
shEPS8L3#1R	AATTCAAAAAGGAGCCAGCTACTTCGCATAACTCGAGTTATGCGAAGTAGCTGGCTCC
shEPS8L3#2F	CCGGGGAGCCAGCTACTTCGCATAACTCGAGTTATGCGAAGTAGCTGGCTCCTTTTTG
shEPS8L3#2R	AATTCAAAAAGGAGCCAGCTACTTCGCATAACTCGAGTTATGCGAAGTAGCTGGCTCC
shKLF5#1F	CCGGCCAGAGACCGTGCGTAACACTCGAGTGTTACGCACGGTCTCTGGTTTTTG
shKLF5#1R	AATTCAAAAACCAGAGACCGTGCGTAACACTCGAGTGTTACGCACGGTCTCTGG
shKLF5#2F	CCGGGAACTGGCCTCTACAAATCCTCGAGGATTTGTAGAGGCCAGTTCTTTTTG
shKLF5#2R	AATTCAAAAAGAACTGGCCTCTACAAATCCTCGAGGATTTGTAGAGGCCAGTTC
shMYO1A#1F	CCGGTGCCATCCACAAACGTCTTAGCTCGAGCTAAGACGTTTGTGGATGGCATTTTTG
shMYO1A#1R	AATTCAAAAATGCCATCCACAAACGTCTTAGCTCGAGCTAAGACGTTTGTGGATGGCA
shMYO1A#2F	CCGGCCGAAAGAATTATCGCAAATACTCGAGTATTTGCGATAATTCTTTCGGTTTTTG
shMYO1A#2R	AATTCAAAAACCGAAAGAATTATCGCAAATACTCGAGTATTTGCGATAATTCTTTCGG
shSOX9#1F	CCGGCTCCACCTTCACCTACATGAACTCGAGTTCATGTAGGTGAAGGTGGAGTTTTTG
shSOX9#1R	AATTCAAAAACTCCACCTTCACCTACATGAACTCGAGTTCATGTAGGTGAAGGTGGAG
shSOX9#2F	CCGGGGAACAACCCGTCTACACACTCGAGTGTGTAGACGGGTTGTTCCTTTTTG
shSOX9#2R	AATTCAAAAAGGAACAACCCGTCTACACACTCGAGTGTGTAGACGGGTTGTTCC
shSP1#1F	CCGGGGAGTGATGCCTAATATTCCTCGAGGAATATTAGGCATCACTCCTTTTTG
shSP1#1R	AATTCAAAAAGGAGTGATGCCTAATATTCCTCGAGGAATATTAGGCATCACTCC
shSP1#2F	CCGGGCCAATAGCTACTCAACTACTCGAGTAGTTGAGTAGCTATTGGCTTTTTG
shSP1#2R	AATTCAAAAAGCCAATAGCTACTCAACTACTCGAGTAGTTGAGTAGCTATTGGC
shNTC-F	CCGGTGGTTTACATGTTTTCTGACTCGAGTCAGAAAACATGTAAACCATTTTTG
shNTC-R	AATTCAAAAATGGTTTACATGTTTTCTGACTCGAGTCAGAAAACATGTAAACCA
For RT-qPCR	
EpCAM-qF	CCATGTGCTGGTGTGTGAAC
EpCAM-qR	ACGCGTTGTGATCTCCTTCT
CD13-qF	CTGTGAGCCAGTCTAGTTCCTGAT
CD13-qR	CATCGAGAGCTTCTGCTCATCT
CD24-qF	GCTCCTACCCACGCAGATTT
CD24-qR	GAGACCACGAAGAGACTGGC
KLF5-qF	AAGGAGTAACCCCGATTTGG
KLF5-qR	TGGCTTTTCACCAGTGTGAG
SOX9-qF	AGGAAGCTCGCGGACCAGTAC
SOX9-qR	GGTGGTCCTTCTTGTGCTGCAC
EPS8L3-qF	CTGCTACAGTCCTGTCTAAGCC
EPS8L3-qR	GAGAATGTGGGTTGGTAGGGCA
MYO1A-qF	CCTACTGGGGCTGAAGAACA
MYO1A-qR	GGGGACACTCTGGGGATATG
HPRT1-qF	CTTTGCTGACCTGCTGGATT
HPRT1-qR	CTGCATTGTTTTGCCAGTGT

West Cluster (UW 17-056) and informed consents from patients. The HCC tumor samples were freshly collected and dissociated as described previously[2] (Figure 1*A*). In brief, tumor tissue was cut into smaller pieces and further minced in medium (Dulbecco modified Eagle medium [DMEM]-F12, Invitrogen Gibco, Waltham, MA) with 16 μmol/L ROCK inhibitor Y-27632 (Selleckchem, Houston, TX). The content was transferred to gentleMACS C tube (Miltenyi Biotec, Germany), and the dissociation was carried out in the presence of DNase (Roche, Switzerland) and liberase (Roche) by the automated gentleMACS dissociator (Miltenyi Biotec) using the built-in program specific for dissociating human tumor tissues. The C tube was incubated at 37°C for 5 minutes in between steps of the dissociation program. The content was finally filtered through cell strainer with 100-μm pore size, followed by centrifugation at $\sim$100*g* for 4 minutes to harvest the cell pellet. The cell pellet was washed in medium and centrifuged for 2–3 times until the pellet was not red or pink in color. The cell pellet was resuspended in DMEM-F12 medium with the cell concentration and viability determined by

Table 6. Open Reading Frame Used in This Study

Gene name	Sequence ID	Cloning site
SP1	NM_138473	Hind III/EcoRI

trypan blue staining. The derived cells were then subjected to immunostaining for flow cytometry and FACS as described below.

Immunostaining for Flow Cytometry and FACS

About 1×10^5 dissociated, live HCC cells were centrifuged per flow tube, and the cell pellet was resuspended in FACS buffer (phosphate-buffered saline with 2% fetal bovine serum [FBS]) at a ratio of 40 μL per 1×10^5 cells. Five microliters of the respective phycoerythrin and BV421 or VioBlue-conjugated antibodies for flow cytometry (Becton Dickinson, Franklin Lakes, NJ and Miltenyi Biotec, Germany) and 7AAD (Becton Dickinson) dye were added and incubated in the dark for a total period of around 1 hour and 20 minutes, respectively. The lists of antibodies used can be found in Table 4. The cells were finally washed once in FACS buffer and resuspended at a final concentration of 2×10^6/mL for subsequent cell sorting. FACS was carried out at the HKU Faculty Core Facility as previously described[1]; 7AAD-positive cells (dead cells), CD45-positive, and multiplet cells were gated out. Only 7AAD-negative (viable cells) singlet cells negative for CD45 were further gated for determining the concerned fluorochrome signal intensities for the respective CSC marker in respective flow tube. Immunoglobulin (IgG) controls of respective fluorochromes were used to determine the threshold of the signal intensity to define marker-positive cells by regarding around 1% of cells with the highest intensity as having non-specific binding of the concerned antibody. The population with positive staining and the 20% highest intensity of the entire live CD45-negative singlet cell population was regarded as the marker-high cells, whereas the population with 2-fold lower intensity or negative staining for the concerned fluorochrome was regarded as marker-low cells. The respective marker-high and marker-low cells were sorted into the respective receiving tubes containing FACS buffer (phosphate-buffered saline with 2% FBS). In case of need for comparison in analysis, the tumor bulk cells that were the viable singlet cells were also collected in separate receiving tube. The collected cells were finally centrifuged at 3000 rpm to obtain the cell pellet for subsequent downstream RNA extraction and transcriptome sequencing and analysis.

RNA Extraction and Transcriptome Sequencing and Analysis

The sorted cell pellets were subjected to RNA extraction by using the RNA extraction kit (Sigma-Aldrich, St Louis, MO). In brief, the pellets were resuspended in the lysis buffer from the kit and vortexed briefly before adding 100% ethanol to vortex briefly according to the kit manufacturer's instructions. The content was passed through a spin column and then subjected to on-column DNase treatment (Qiagen, Germany, catalogue no. 79254) for 10 minutes at room temperature before washing by the wash buffer provided in the kit for 3 times according to the manufacturer's instructions. The RNA was finally eluted in 10 μL elution buffer of the kit according to the instructions. The RNA samples were then subjected to bioanalysis by Centre for PanorOmic Sciences (CPOS) of the Faculty of Medicine in HKU to determine the RIN. Satisfactory quality RNA (RIN $>$6.0) was then subjected for RNA sequencing by CPOS of the Faculty in HKU, as previously reported.[1]

Library Preparation and Transcriptome Sequencing

All of the libraries were prepared on the basis of the protocols of SMART-Seq v4 Ultra Low Input RNA Kit for Sequencing (Clontech), Nextera XT DNA Sample Prep Kit (Illumina), and Nextera XT Index Kit (Illumina). Manufacturer's protocol was followed, and 1 ng of total RNA was used as starting material. Briefly, full-length double-stranded cDNA was generated. cDNA fragments with adaptors were generated by tagmentation reaction. Adaptor-ligated libraries were generated in 50 μL reaction volume with 11 cycles of PCR. The enriched libraries were validated by Agilent Bioanalzyer, Qubit, and qPCR for quality control analysis. The libraries were denatured and diluted to optimal concentration. Illumina NovaSeq 6000 was used for paired-end 151 bp sequencing.

Bioinformatics Analysis

Transcriptome sequencing data were similarly analyzed as previously described.[1,2] In brief, sequencing reads were aligned to reference human genome (hg38) by HISAT2. Transcripts were assembled by StringTie, and the expression level of individual genes was identified as fragments per kilobase per million (FPKM). We also counted the raw read counts of genes using featureCounts and subjected them for differential gene expression analysis by edgeR. DEGs were selected as having differential gene expression P value $<$.05, fold change $>$1.5, and median FPKM $>$0.5.

Multicolor Immunofluorescence Imaging

FFPE tissues of corresponding HCC cases were cut at 5-μm thickness. Multicolor immunofluorescence staining was performed manually by using Opal Polaris 7 color IHC kit (NEL797001KT; PerkinElmer, Waltham, MA), according to the manufacturer's instructions. The slides were stained with CD13 (Abcam Ab108382, 1:1000, room temperature, 90 minutes) with Opal 480 fluorophore, EpCAM (Abcam Ab223582, 1:250, room temperature, 90 minutes) with Opal 570 fluorophore, and CD24 (Abcam Ab214231, 1:250, room temperature, 90 minutess) with Opal 620 Fluorophore, and then with DAPI at 5 μg/mL for 5 minutes before being mounted with antifade mounting medium (H1700, Vector Laboratories, Burlingame, CA). Slides were scanned using Vectra Polaris Automated Quantitative Pathology Imaging System

(PerkinElmer) at CPOS of the Faculty at 40× resolution. Final images were then processed by using Image J (FUJI, Japan).

Cell Lines and Culture

PLC/PRF/5, Huh7, Hep3B, and 293FT cells were cultured in DMEM-HG (Invitrogen Gibco) supplemented with 10% FBS, 1% penicillin, and 1% streptomycin. MHCC-97L cells were cultured in the above mentioned medium supplemented with 1 mmol/L sodium pyruvate (NaPy). Cell lines were cultured in 37°C and 5% CO_2 incubator.

HCC cell lines PLC/PRF/5 (CRL-8024) and Hep3B (HB-8064) were obtained from American Type Culture Collection. HCC cell line Huh-7 (JCRB0403) was obtained from JCRB Cell Bank. MHCC-97L was a gift from Liver Cancer Institute, Fudan University. Human embryonic kidney cell line 293FT (R70007) was obtained from Invitrogen (Carlsbad, CA). All cell cultures were negative for Mycoplasma contamination.

Stable Knockdown Clone Establishment and Quantitative Real-Time Polymerase Chain Reaction

Stable knockdown clones were established by lentiviral approach. Oligos for subcloning shRNAs sequences into pLKO.1-Puro shRNA expression vector purchased from Dharmacon (Lafayette, CO) are listed in Table 5. The shRNA vectors were transfected into 293FT cells using Lipofectamine 2000 (Invitrogen), according to the MISSION Lentiviral Packaging System (Sigma-Aldrich) manufacturer's protocol. For viral packaging, the viral particles containing shRNA were transduced into respective HCC cell lines to establish the shRNA stably expressing cells. Total RNA was extracted by Trizol (Invitrogen), and cDNA was synthesized by reverse transcription kit (Invitrogen). Real-time (RT)-qPCR was used by using ABI Power SYBR Green master mix and detected by ABI QuantStudio 5 Real-Time PCR System (Applied Biosystems, Foster City, CA). Primer sequences are listed in Table 5.

Sphere Formation Assays

Cells were suspended in 0.25% methyl cellulose in serum-free DMEM/F12 in wells precoated with 1% poly-HEMA to form spheres in the presence of EGF, fibroblast growth factor, insulin, and B-27 supplement. At end point, the numbers of spheres greater than 100 μm in diameter were counted. Experiments were done thrice independently.

Promoter Cloning, Reporter Assays, and ChIP Assays

Huh-7 cells were transfected with different combinations of plasmids using Lipofectamine 3000 (Invitrogen) according to the manufacturer's protocol. The reporter plasmids used included the constructs for wild-type, -51 mutant, -22 mutant, and -51, -22 mutant promoters for EPS8L3. Open reading frame for SP1 was subcloned into pcDNA3.1+Neo expression vectors (details listed in Table 6). pRL-PGK was used as an internal control. Twenty-four hours after transfection, firefly luciferase and Renilla luciferase activities were measured by Dual Luciferase Reporter assay system (Promega, Madison, WI) according to the manufacturer's protocol. Transfection efficiency was normalized with the Renilla luciferase activity. Experiments were done at least thrice independently. ChIP assays were performed as described before[24] using qPCR primers as listed in Table 5.

Western Blot Analysis

Proteins in cell lysate were separated in sodium dodecyl sulfate-polyacrylamide gel electrophoresis for Western blot analysis. List of antibodies can be found in Table 4.

Statement of Ethics

This study protocol was reviewed and approved by Institutional Review Board of the University of Hong Kong/Hospital Authority Hong Kong West Cluster (HKU/HA HKW IRB), approval number [UW 17-056]. Written informed consent was obtained from participating patients.

References

1. Ho DW, Tsui YM, Sze KM, et al. Single-cell transcriptomics reveals the landscape of intra-tumoral heterogeneity and stemness-related subpopulations in liver cancer. Cancer Letters 2019;459:176–185.
2. Ho DW, Tsui YM, Chan LK, et al. Single-cell RNA sequencing shows the immunosuppressive landscape and tumor heterogeneity of HBV-associated hepatocellular carcinoma. Nat Commun 2021;12:3684.
3. Zhang Q, Lou Y, Yang J, et al. Integrated multiomic analysis reveals comprehensive tumour heterogeneity and novel immunophenotypic classification in hepatocellular carcinomas. Gut 2019;68:2019–2031.
4. Zheng H, Pomyen Y, Hernandez MO, et al. Single-cell analysis reveals cancer stem cell heterogeneity in hepatocellular carcinoma. Hepatology 2018;68:127–140.
5. Liao WY, Hsu CC, Chan TS, et al. Dishevelled 1-regulated superpotent cancer stem cells mediate Wnt heterogeneity and tumor progression in hepatocellular carcinoma. Stem Cell Rep 2020;14:462–477.
6. Haraguchi N, Ishii H, Mimori K, et al. CD13 is a therapeutic target in human liver cancer stem cells. J Clin Invest 2010;120:3326–3339.
7. Lee TK, Castilho A, Cheung VCH, et al. CD24(+) liver tumor-initiating cells drive self-renewal and tumor initiation through STAT3-mediated NANOG regulation. Cell Stem Cell 2011;9:50–63.
8. Medema JP. Cancer stem cells: the challenges ahead. Nat Cell Biol 2013;15:338–344.
9. Ma S, Chan K, Hu L, et al. Identification and characterization of tumorigenic liver cancer stem/progenitor cells. Gastroenterology 2007;132:2542–2556.
10. Ma S, Lee TK, Zheng BJ, et al. CD133+ HCC cancer stem cells confer chemoresistance by preferential expression of the Akt/PKB survival pathway. Oncogene 2008;27:1749–1758.

11. Yamashita T, Ji J, Budhu A, et al. EpCAM-positive hepatocellular carcinoma cells are tumor-initiating cells with stem/progenitor cell features. Gastroenterology 2009;136:1012–1024.
12. Sun Y, Xu Y, Yang X, et al. Circulating stem cell-like epithelial cell adhesion molecule-positive tumor cells indicate poor prognosis of hepatocellular carcinoma after curative resection. Hepatology 2013;57:1458–1468.
13. Asai R, Tsuchiya H, Amisaki M, et al. CD44 standard isoform is involved in maintenance of cancer stem cells of a hepatocellular carcinoma cell line. Cancer Med 2019;8:773–782.
14. Khosla R, Rastogi A, Ramakrishna G, et al. EpCAM+ liver cancer stem-like cells exhibiting autocrine Wnt signaling potentially originate in cirrhotic patients. Stem Cells Transl Med 2017;6:807–818.
15. Lee TK, Cheung VC, Lu P, et al. Blockade of CD47-mediated cathepsin S/protease-activated receptor 2 signaling provides a therapeutic target for hepatocellular carcinoma. Hepatology 2014;60:179–191.
16. Wu J, Zhu P, Lu T, et al. The long non-coding RNA LncHDAC2 drives the self-renewal of liver cancer stem cells via activation of Hedgehog signaling. J Hepatol 2019;70:918–929.
17. Yamashita T, Honda M, Nakamoto Y, et al. Discrete nature of EpCAM+ and CD90+ cancer stem cells in human hepatocellular carcinoma. Hepatology 2013;57:1484–1497.
18. Nio K, Yamashita T, Okada H, et al. Defeating EpCAM(+) liver cancer stem cells by targeting chromatin remodeling enzyme CHD4 in human hepatocellular carcinoma. J Hepatol 2015;63:1164–1172.
19. Lai HC, Chung WM, Chang CM, et al. Androgen receptor enhances the efficacy of sorafenib against hepatocellular carcinoma through enriched EpCAM stemness. Anticancer Res 2020;40:1285–1295.
20. Sakabe T, Azumi J, Umekita Y, et al. Prognostic relevance of miR-137 in patients with hepatocellular carcinoma. Liver Int 2017;37:271–279.
21. Xu Q, Xu HX, Li JP, et al. Growth differentiation factor 15 induces growth and metastasis of human liver cancer stem-like cells via AKT/GSK-3beta/beta-catenin signaling. Oncotarget 2017;8:16972–16987.
22. Takai A, Dang H, Oishi N, et al. Genome-wide RNAi screen identifies PMPCB as a therapeutic vulnerability in EpCAM(+) hepatocellular carcinoma. Cancer Res 2019;79:2379–2391.
23. Russ A, Hua AB, Montfort WR, et al. Blocking "don't eat me" signal of CD47-SIRPalpha in hematological malignancies, an in-depth review. Blood Rev 2018;32:480–489.
24. Tian L, Zhao L, Sze KM, et al. Dysregulation of RalA signaling through dual regulatory mechanisms exerts its oncogenic functions in hepatocellular carcinoma. Hepatology 2022;76:48–65.
25. Sze KM, Wong KL, Chu GK, et al. Loss of phosphatase and tensin homolog enhances cell invasion and migration through AKT/Sp-1 transcription factor/matrix metalloproteinase 2 activation in hepatocellular carcinoma and has clinicopathologic significance. Hepatology 2011;53:1558–1569.
26. Han X, Wang Y, Pu W, et al. Lineage tracing reveals the bipotency of SOX9(+) hepatocytes during liver regeneration. Stem Cell Rep 2019;12:624–638.
27. Leung CO, Mak WN, Kai AK, et al. Sox9 confers stemness properties in hepatocellular carcinoma through Frizzled-7 mediated Wnt/beta-catenin signaling. Oncotarget 2016;7:29371–29386.
28. Maehara O, Sato F, Natsuizaka M, et al. A pivotal role of Kruppel-like factor 5 in regulation of cancer stem-like cells in hepatocellular carcinoma. Cancer Biol Ther 2015;16:1453–1461.
29. Zeng CX, Tang LY, Xie CY, et al. Overexpression of EPS8L3 promotes cell proliferation by inhibiting the transactivity of FOXO1 in HCC. Neoplasma 2018;65:701–707.
30. Xuan Z, Zhao L, Li Z, et al. EPS8L3 promotes hepatocellular carcinoma proliferation and metastasis by modulating EGFR dimerization and internalization. Am J Cancer Res 2020;10:60–77.
31. Li P, Hu T, Wang H, et al. Upregulation of EPS8L3 is associated with tumorigenesis and poor prognosis in patients with liver cancer. Mol Med Rep 2019;20:2493–2499.
32. Chen B, Pan Y, Xu X, et al. Inhibition of EPS8L3 suppresses liver cancer progression and enhances efficacy of sorafenib treatment. Biomed Pharmacother 2020;128:110284.
33. Tyska MJ, Mooseker MS. MYO1A (brush border myosin I) dynamics in the brush border of LLC-PK1-CL4 cells. Biophys J 2002;82:1869–1883.
34. Lin P, Zhao C, Li Z, et al. Sp1 is involved in regulation of cystathionine γ-lyase gene expression and biological function by PI3K/Akt pathway in human hepatocellular carcinoma cell lines. Cell Signal 2012;24:1229–1240.
35. Tian LY, Smit DJ, Jücker M. The role of PI3K/AKT/mTOR signaling in hepatocellular carcinoma metabolism. Int J Mol Sci 2023;24:2652.

Received October 10, 2023. Accepted May 7, 2024.

Correspondence
Address correspondence to: Irene Oi-Lin Ng, MD, PhD, Room 7-13, Block T, Queen Mary Hospital, Pokfulam, Hong Kong. e-mail: iolng@hku.hk.

Acknowledgments
The authors thank the Centre for PanorOmic Sciences (CPOS) of the LKS Faculty of Medicine of the University of Hong Kong for providing the facilities and services for the FAC-sorting, flow cytometry, and transcriptome analyses. Graphical abstract was created with BioRender.com.

CRediT Authorship Contributions

Yu Man Tsui (Data curation: Lead; Formal analysis: Lead; Investigation: Lead; Methodology: Lead; Project administration: Lead; Supervision: Lead; Validation: Lead; Visualization: Lead; Writing – original draft: Lead; Writing – review & editing: Lead)

Daniel Wai-Hung Ho (Data curation: Lead; Formal analysis: Lead; Investigation: Lead; Methodology: Lead; Project administration: Lead; Software: Lead; Supervision: Lead; Validation: Lead; Visualization: Lead; Writing – original draft: Lead; Writing – review & editing: Lead)

Karen Man-Fong Sze (Data curation: Lead; Formal analysis: Lead; Investigation: Lead; Methodology: Lead; Project administration: Lead; Supervision: Lead; Validation: Lead; Visualization: Lead; Writing – original draft: Lead; Writing – review & editing: Lead)

Joyce Man-Fong Lee (Data curation: Supporting),

Eva Lee (Data curation: Supporting)

Qingyang Zhang, PhD (Formal analysis: Supporting)

Gary Cheuk-Hang Cheung (Methodology: Supporting)

Chung-Ngai Tang (Data curation: Supporting)
Victor Wai-Lun Tang (Data curation: Supporting)
Elaine Tin-Yan Cheung (Data curation: Supporting)
Irene Lai-Oi Lo (Data curation: Supporting)
Albert Chi-Yan Chan (Data curation: Supporting)
Tan-To Cheung (Data curation: Supporting)
Irene O. L. Ng, MD, PhD (Conceptualization: Lead; Data curation: Lead; Funding acquisition: Lead; Investigation: Lead; Methodology: Lead; Project administration: Lead; Resources: Lead; Supervision: Lead; Writing – original draft: Lead; Writing – review & editing: Lead)

Conflicts of interest

The authors disclose no conflicts.

Funding

Supported by the Hong Kong Research Grants Council Theme-based Research Scheme (T12-704/16-R and T12-716/22-R), Innovation and Technology Commission grant for State Key Laboratory of Liver Research (ITC PD/17-9), National Natural Science Foundation of China (81872222, 82203234, and 82394451), and University Development Fund and Seed Fund for Basic Research (2201101565) of The University of Hong Kong. Irene O. L. Ng is Loke Yew Professor in Pathology.